XIV National School on Superconductivity, Ostrów Wielkopolski, October 13–17, 2009

Comparative Study of the Electronic Structures of Fe_3O_4 and Fe_2SiO_4

P. Piekarz*, A.M. Oleś and K. Parlinski

Institute of Nuclear Physics, Polish Academy of Sciences,E. Radzikowskiego 152, PL-31-342 Kraków, Poland

The electronic properties of two spinels Fe_3O_4 and Fe_2SiO_4 are studied by the density functional theory. The local Coulomb repulsion U and the Hund exchange J between the $3d$ electrons on iron are included. For $U = 0$, both spinels are half-metals, with the minority t_{2g} states at the Fermi level. Magnetite remains a metal in a cubic phase even at large values of U. The metal–insulator transition is induced by the X_3 phonon, which lowers the total energy and stabilizes the charge-orbital ordering. Fe_2SiO_4 transforms to a Mott insulating state for $U > 2$ eV with a gap $\Delta_g \sim U$. The antiferromagnetic interactions induce the tetragonal distortion, which releases the geometrical frustration and stabilizes the long-range order. The differences of electronic structures in the high-symmetry cubic phases and the distorted low-symmetry phases of both spinels are discussed.

PACS numbers: 71.27.+a, 71.30.+h, 71.38.−k

1. Introduction

In transition-metal spinels, magnetic, charge, and orbital interactions are strongly affected by the crystal geometry. A special character of spinels is associated with the arrangement of cations in the octahedrally coordinated sites forming a pyrochlore lattice. Consisting of the corner-sharing tetrahedra, this crystal structure causes the geometrical frustration of magnetic interactions and makes the electronic ground state highly degenerate [1]. In such cases, the system may remain in a disordered state like a quantum spin liquid or spin ice even at low temperatures [2]. It makes also the electronic state very susceptible to lattice distortion, which lifts the degeneracy and drives the structural phase transition.

Spinels have a general formula AB_2O_4 and at room temperature crystallize in the cubic $Fd\bar{3}m$ (O_h^7) symmetry (Fig. 1). In a normal spinel, the A and B cations occupy the tetrahedral and octahedral positions, respectively. The B sites create the atomic chains along the [110] and [1$\bar{1}$0] directions. In the most common cases, the valence state for the A site is 2+ and for the B site 3+ (*e.g.* in $MgAl_2O_4$). The 4+ valence state for the A site exists only in the high-pressure forms of olivines (Fe_2SiO_4, Co_2SiO_4). In inverse spinels, the A atoms occupy half of the octahedral sites, while the B ones are shared equally by the octahedral and tetrahedral sites. Fe_3O_4 is classified as the inverse spinel due to mixed valency of iron ions in the octahedral sites (2+/3+).

Depending on the type of cations in the octahedral sites, transition-metal spinels exhibit various types of ordered phases at low temperatures [3]. One observes antiferromagnetic (AF) phases (MgV_2O_4) [4],

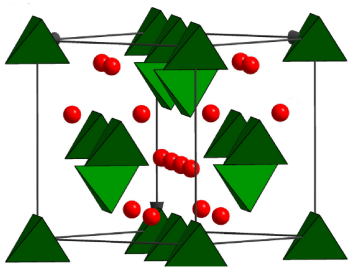

Fig. 1. The spinel structure: the octahedral B sites are represented by red balls and the AO_4 units are plotted as green tetrahedra.

charge ordering ($CuIr_2S_4$) [5], metal–insulator transitions ($MgTi_2O_4$) [6], or spin-Peierls transitions ($ZnCr_2O_4$) [7]. Crystal distortions in these phase transitions are associated with different electron–lattice couplings. In $ZnMn_2O_4$, the symmetry reduction to the tetragonal space group $I4_1/amd$ is driven by the Jahn–Teller effect. The tetragonal distortion in $ZnCr_2O_4$ observed at $T_N = 12.5$ K induces the spin gap in magnetic excitations similarly as in the one-dimensional spin-Peierls systems. The metal–insulator transition in $MgTi_2O_4$ is associated with the spin-singlet formation and dimerization of the atomic bonds [8].

The Verwey transition in Fe_3O_4 has a very unique character and its microscopic origin has been intensively studied for more than 60 years. Verwey proposed that a discontinuous drop of the electrical conductivity at $T_V = 122$ K is associated with the ordering of the Fe^{3+} and Fe^{2+} ions in the octahedral sites [9]. According to this scenario, the conductivity increases above T_V due to higher mobility of electrons fluctuating between the Fe sites. At T_V, electron movement freezes out and the

* corresponding author; e-mail: piekarz@wolf.ifj.edu.pl

charge ordering stabilized by the electrostatic forces develops. However, this simple picture was not confirmed by more recent studies. Firstly, Anderson demonstrated that in the spinel geometry the energy difference between a short-range and long-range order is very small and therefore typical order–disorder mechanism is unlikely [1]. Secondly, the crystallographic studies revealed the monoclinic deformation below $T_{\rm V}$, which is inconsistent with the Verwey model [10]. The diffraction measurements support only the fractional charge ordering with small differences of charges [11, 12]. Finally, the theoretical studies demonstrated the importance of local Coulomb interactions in the $3d$ states on iron, which induces the charge-orbital ordering in the monoclinic phase [13]. In our studies, we developed the mechanism of the Verwey transition based on the interplay between the electron correlations and the electron–phonon interaction [14–16].

Spinels containing Si atoms belong to a separate group of minerals stable only under high pressure, as realized in the Earth upper mantle. Fe_2SiO_4, which is the end-member of geologically important group of olivines $(Mg,Fe)_2SiO_4$, can be obtained from magnetite by replacing the Fe atom at the A site by the Si atom. The experimental information on the electronic properties of this mineral is very limited. The heat capacity measurement revealed the peak at $T_{\rm N} = 11.8$ K, most probably associated with the paramagnetic–antiferromagnetic transition [17]. Above $T_{\rm N}$, a paramagnetic state is consistent with the Mössbauer measurements [18]. In the previous study, we have analyzed the electronic structure of Fe_2SiO_4 using the density functional theory (DFT) [19]. We found that the insulating state results from the local Hubbard interaction U included within the generalized gradient approximation in the so-called GGA+U approach. In addition, we revealed that the AF interactions induces the tetragonal distortion, removing the geometrical frustration.

In this paper, we compare the electronic properties of Fe_3O_4 and Fe_2SiO_4, analyzing in detail the changes induced by the Hubbard interaction U and crystal distortions. For Fe_2SiO_4, we investigate the effect of high pressure on the electronic structure.

The paper is organized as follows. The details of the calculation method are presented in Sect. 2. Electronic structures of Fe_3O_4 and Fe_2SiO_4 are reported and analyzed separately for the high symmetry phase (Sect. 3.1) and low symmetry phase (Sect. 3.2). Discussion of the results and a short summary are presented in Sect. 4.

2. Calculation method

The electronic and crystal structures of both spinels were optimized within the GGA+U method using the VASP code [20]. The wave functions were obtained by the full-potential projector augmented-wave method [21]. The basis included the following valence electron configurations: Fe:$3d^64s^2$, Si:$3s^23p^2$, and O:$2s^22p^4$. To compare the effects induced by the local electron interactions in the $3d$ states on iron, the same values of the Coulomb and Hund exchange parameters were chosen: $U = 4$ eV and $J = 0.8$ eV. The repulsion energy U was taken from the constrained DFT calculations [22] and J was obtained from the atomic values of the Racah parameters for Fe^{2+} ions [23]: $B = 0.131$ eV and $C = 0.484$ eV. It is reasonable to assume that the Coulomb interaction parameters $\{U, J\}$ are the same in both Fe_3O_4 and Fe_2SiO_4 systems in their insulating phases, as one expects that the screening of the Coulomb interaction should be rather similar. However, we cannot exclude that the Coulomb parameter U changes in the magnetite at the Verwey transition, when the metallic state is transformed into an insulating one (this effect was not considered in the theory until now).

The calculations for the cubic symmetry $Fd\bar{3}m$ were performed in the $a \times a \times a$ supercell and for the monoclinic phase $P2/c$ of magnetite in the $a/\sqrt{2} \times a/\sqrt{2} \times 2a$ cell, both with 56 atoms. The electronic structures were obtained for the fully relaxed crystals. For Fe_2SiO_4, the results were obtained at two hydrostatic pressures $p = 0$ and $p = 20$ GPa. The latter value corresponds to a stable spinel phase existing only under high-pressure conditions.

3. Electronic structures

3.1. High-symmetry phases

In the case of the iron-based spinels, the electronic structures can be well understood starting from the electron configurations of the Fe^{2+} and Fe^{3+} ions. In Fe_2SiO_4, the iron atoms have a uniform electron distribution corresponding to the 2+ charge valency. The octahedral sites in magnetite have the mixed valence configuration with an average charge 2.5+. Due to the Hund exchange both ionic configurations correspond to the high spin states Fe^{2+}: $t^3_{2g\uparrow}t_{2g\downarrow}e^2_{g\uparrow}$ ($S = 2$) and Fe^{3+}: $t^3_{2g\uparrow}e^2_{g\uparrow}$ ($S = 5/2$). The splitting of the $3d$ states into the t_{2g} and e_g orbitals is induced by the crystal field, which is much larger at the octahedral sites than at the tetrahedral ones. The exchange coupling causes the splitting of the majority up-spin and minority down-spin states and shifts one type of the states with respect to the other. Consequently only the down-spin states occupy the energy levels close to the Fermi energy ($E_{\rm F}$) [22].

In Fig. 2, we compare the electronic density of states (DOS) in these compounds for $U = J = 0$. If the local electron interactions are neglected, the ground states of both spinels are half-metallic with the minority down-spin t_{2g} states at $E_{\rm F}$. These states come only from the Fe atoms at the octahedral sites. Neither the $3d$ states on the Fe(A) atoms in magnetite nor the s and p states participate in the electron transport. Similarly to the Fe(B) states, the up-spin and down-spin states at the Fe(A) sites are splitted by the exchange coupling. All the down-spin states are occupied, while the up-spin states are empty, so the magnetic moments on the A and B

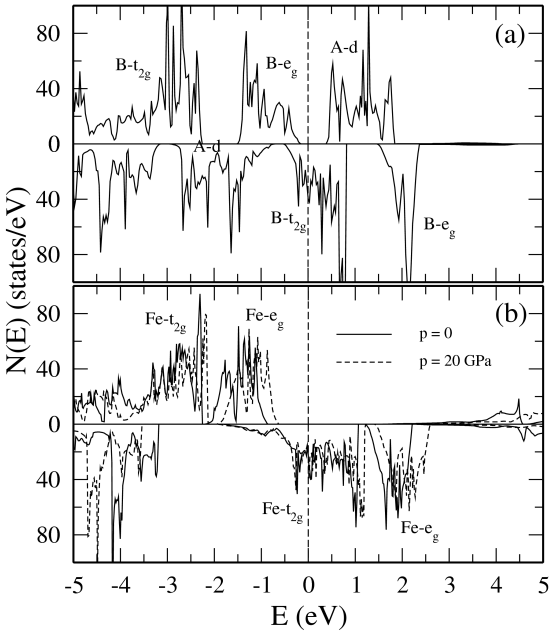

Fig. 2. Electronic structure of (a) Fe_3O_4 at $p = 0$ pressure and (b) Fe_2SiO_4 obtained in the cubic $Fd\bar{3}m$ symmetry for two pressure values, $p = 0$ (solid lines) and $p = 26$ GPa (dashed lines), and for $U = J = 0$.

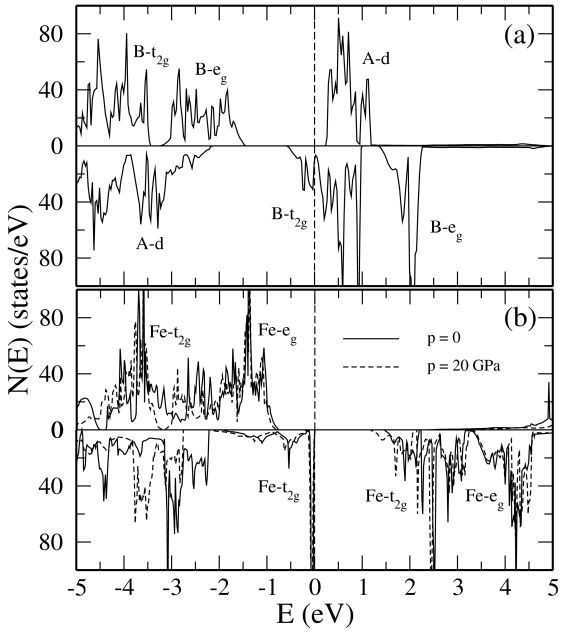

Fig. 3. The same as in Fig. 2 for $U = 4$ eV and $J = 0.8$ eV.

sites have the opposite directions generating the ferrimagnetic order in magnetite. The half-metallic ground state of magnetite agrees with the properties of the high-symmetry phase indicating that the local Coulomb interactions do not play important role at high temperatures.

Without the Hubbard interaction, the metallic ground state of Fe_2SiO_4 has the ferromagnetic (FM) order with the magnetic moment on iron equal to 3.57 μ_B. It remains a metal even at high pressures, showing a disagreement with the insulating behavior of this material. As shown in Fig. 2b, the main effect of pressure is to increase the bandwidth due to larger overlap of the $3d$ orbitals. The splitting of the t_{2g} and e_g states also increases because of the stronger crystal field.

In the next step, we compare the changes in the DOSs induced by the on-site interactions U and J, while keeping the cubic symmetry. We allow only for the relaxation of the lattice constant and the internal parameter u. The lattice constants of both crystals increase slightly (less than 1%) because of the larger Coulomb repulsion between electrons [15, 19]. In magnetite, the electronic state does not change much comparing to the uncorrelated case, Fig. 3a. There is an additional shift of the majority up-spin Fe(B) and down-spin Fe(A) states to lower energies due to larger exchange coupling. It increases the magnitudes of magnetic moments on the Fe(A) sites from 3.40 to 3.97 μ_B and on the Fe(B) sites from 3.52 and 3.87 μ_B, improving the agreement with the experiment. The ground state remains metallic even at presence of strong on-site interaction U.

In Fe_2SiO_4, there is a larger electron occupation of the t_{2g} states on the Fe(B) atoms (one electron per one iron site), so the on-site Hubbard interaction U is much more effective than in magnetite. As shown in Fig. 3b, the interaction U has a strong impact on the electronic DOS, inducing the insulating gap at E_F. The gap with the magnitude 1.5 eV separates the occupied down-spin t_{2g} states from the empty ones. The insulating state is generated by the inter-orbital Hubbard interaction with the effective energy $U_{\rm eff} = U - J$ (note that U is here an average value of local Coulomb interaction for different electron pairs, as usually assumed in the local density approximation supplemented by local electron–electron interactions (LDA+U) [13, 24]), so the magnitude of the gap can be estimated from the formula

$$\Delta_g = U_{\rm eff} - \frac{W}{2}\,, \tag{1}$$

where W is the width of the t_{2g} band. For $W \approx 3$ eV, we get $\Delta_g \approx 1.7$ eV, which corresponds very well with the obtained gap. At high pressure, the insulating gap decreases to 1.2 eV, and this effect can be easily understood from Eq. (1) — under increasing pressure the band width W increases, thus reducing the value of the gap.

The results obtained for a cubic phase with a realistic value of U reveal a fundamental difference between these two spinel structures. On the one hand, Fe_2SiO_4 behaves like a Mott insulator with the gap $\Delta_g \sim U$, and the local Hubbard interaction is crucial to reproduce the electronic properties of this material. On the other hand, the on-site interaction U alone does not induce the insulating state in magnetite, and in the cubic symmetry this material remains in a metallic state. This may be concluded from the behavior at high temperatures, in particular

from a relatively high conductivity. This theoretical result indicates that Fe_3O_4 is not a Mott insulator, and its non-metallic state at low temperatures has a different origin.

3.2. Low-symmetry phases

The phase transitions observed in the discussed materials at low temperatures have fundamentally different nature. The Verwey transition involves both the charge and orbital degrees of freedom, and their ordering below T_V is stabilized by the monoclinic distortion [13]. Using the group theory, we found that the low-symmetry phase results from the condensation of two phonons (order parameters) with the symmetries Δ_5 and X_3 [14]. The strength of the electron–phonon coupling strongly depends on the Hubbard interaction U, which induces the antiferro-orbital ordering and splitting of the t_{2g} states at the Fermi level. Without the lattice distortion, the electronic state with orbital polarization is highly degenerate showing a short-range order [25]. We found that the charge-orbital ordering is stabilized by the coupling between the $3d$ electrons and the X_3 phonon [15]. This coupling lowers the total energy of the crystal and induces the metal–insulator transition.

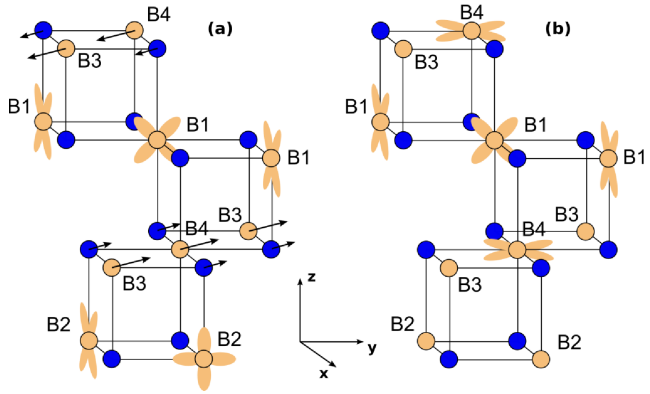

Fig. 4. Orbital ordering induced by: (a) the X_3 mode (the black arrows), and (b) the monoclinic symmetry $P2/c$. Nonequivalent Fe positions are labeled as B1, B2, B3, and B4.

The orbital order of the t_{2g} states with the atom displacements corresponding to the X_3 mode is shown in Fig. 4a. The positions of atoms were generated from the polarization vectors using the PHONON software [26]. Iron atoms occupy 4 different positions in the structure labeled as B_1, B_2, B_3, and B_4. Phonons at the X point are doubly degenerate, so we have chosen only one phonon branch. In the presented case, the displacements of the B_3 and B_4 atoms together with oxygens located in the same plane induce the orbital ordering on the B_1 and B_2 atoms in the nearest neighbor planes. The second order parameter Δ_5 also couples strongly to electrons but it does not induce the gap opening. It generates the crystal distortion which doubles the unit cell in the c direction. These results demonstrate that the cubic phase is not a real ground state of magnetite, and the structural transition to a phase with broken symmetry must occur when temperature is lowered.

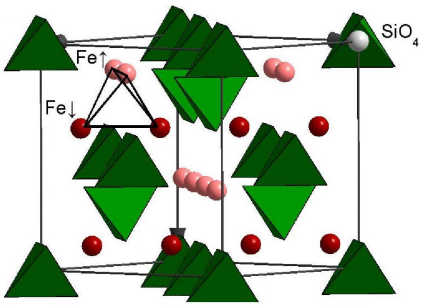

Fig. 5. The AF ordering in Fe_2SiO_4 — light/dark spheres indicate positions of ↑ and ↓ magnetic moments on Fe atoms.

In contrast, the phase transition occurs in Fe_2SiO_4 at much lower temperature $T_N = 11.8$ K, and is driven by the magnetic interactions. We have considered two magnetic configurations with the FM and AF order. We assumed that the magnetic moments in the AF configuration are aligned parallel in the (001) planes, and have opposite (alternating) directions in the subsequent planes along the c axis (see Fig. 5). Instead of the c axis one can choose either a or b direction, so the AF order is triply degenerate in the cubic symmetry. We found that for $U > 2$ eV, there is a change of the ground state from the FM to AF order [19]. This change is driven by the metal–insulator transition at the same value of U. Therefore, the electronic DOS with the FM order presented in Fig. 3b does not correspond to the ground state realized at $U = 4$ eV. We revealed that the AF configuration induces the tetragonal distortion ($a > c$), breaking the cubic symmetry and lowering the total energy. This distortion depends on the Hubbard interaction U and for $U = 4$ eV one finds $c = 0.985a$. The contraction of the crystal along the c axis enhances the superexchange interaction along the AF bonds, while the elongation in the ab plane weakens the one along FM bonds.

The electronic DOSs in the low symmetry phases of both spinels were obtained by full relaxation of the crystal structures without imposing the cubic symmetry constraints. Fe_3O_4 has the monoclinic $P2/c$ symmetry with the doubled lattice constant in the c direction. In this symmetry there are two non-equivalent tetrahedral positions A_1 and A_2 (not shown), and four octahedral sites B_1, B_2, B_3, and B_4, shown in Fig. 4b. The lattice parameters and atomic positions were analyzed in detail in Ref. [15]. Fe_2SiO_4 has the tetragonal $I4_1/amd$ space group.

The electronic structures for the above symmetries are presented in Fig. 6. The insulating gaps in the minority t_{2g} states now exist in both systems. Comparing to the FM phase of Fe_2SiO_4, the gap in the AF phase is

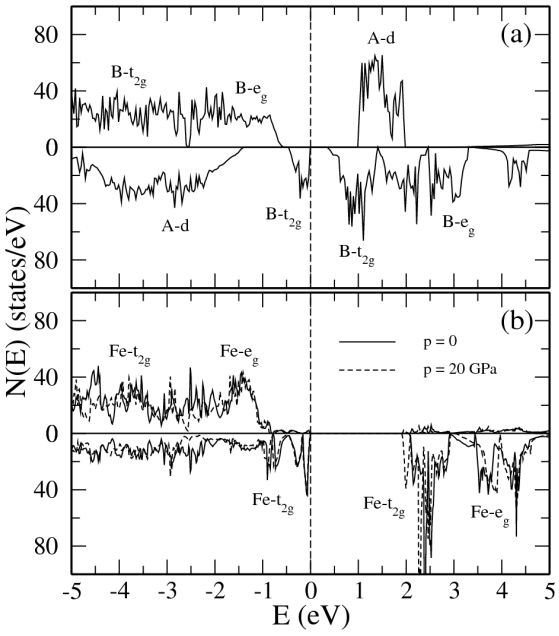

Fig. 6. Electronic structures of (a) the $P2/c$ phase of Fe_3O_4, and (b) the $I4_1/amd$ phase of Fe_2SiO_4. Parameters: $U = 4$ eV and $J = 0.8$ eV.

larger (2 eV). Under pressure, the magnitude of the gap decreases as in the FM case. The gap $\Delta_g = 0.33$ eV obtained in magnetite agrees quite well with the experimental value 0.14 eV [27] and is much smaller than the gap in Fe_2SiO_4. The gap separates the occupied states at the B_1 and B_4 sites from the empty ones at the B_2 and B_3 sites. This explains the origin of the fractional charge ordering in the monoclinic phase. The orbital ordering arises due to the preferential occupation of the t_{2g} states. A schematic plot of the orbital ordering is presented in Fig. 4b. In the B_1 chains, the electrons occupy the d_{xz} and d_{yz} orbitals creating the antiferro-orbital (alternating orbital) order. At the B_4 sites only the d_{xy} orbitals are occupied by electrons.

4. Discussion

The presented results reveal some interesting aspects of two iron-based spinels. As a common feature, the electronic properties of both compounds are strongly affected by the on-site Hubbard interaction U. The interplay of this local Coulomb interaction with a lattice distortion is the driving force of the observed phase transitions, which leads in both spinels to a new ordered phase with a broken cubic symmetry.

In magnetite, this interaction does not lead directly to the insulating phase as in the Mott–Hubbard mechanism. It enhances a natural tendency of the degenerated t_{2g} states to create an orbital ordering. Such state becomes very sensitive to lattice distortion, which by splitting the t_{2g} band opens the insulating gap. This mechanism is similar to the Jahn–Teller effect, however, the lattice distortion in magnetite is much more complex than in simple perovskites, see e.g. Ref. [28]. The structural transition is here induced by two order parameters, which couple to each other and generate the monoclinic phase [14].

Long time ago, Anderson predicted the existence of the short-range order in magnetite on the basis of the simple electrostatic model [1]. There are many signs of such state above the Verwey transition. One of them is the insulating gap that does not close completely at high temperatures [29]. Recently, the resonant X-ray scattering studies revealed that charge-orbital ordering starts to develop about 10 K above T_V [30]. The charge-orbital fluctuations couple to phonons producing the critical diffuse scattering. The neutron studies found the symmetries of lattice distortions associated with these fluctuations. They are the precursors of the order parameters Δ_5 [31] and X_3 [32].

We revealed that the geologically important mineral Fe_2SiO_4-spinel is a Mott insulator. The on-site Hubbard interaction U in the $3d$ states on iron generates the insulating state with the AF order. We suggest that these AF interactions drive the phase transition observed at $T_N = 11.8$ K. Furthermore, we discovered that the AF order induces the tetragonal distortion reducing the cubic $Fd\bar{3}m$ symmetry to its subgroup $I4_1/amd$. This distortion releases the geometrical frustration of the magnetic interaction enabling for the long-range order. In Ref. [19], we estimated the exchange constant J and the Curie–Weiss temperature θ_{CW} using the classical Heisenberg model. The obtained large values of the exchange constant $J = 1.7$ meV and the Curie–Weiss temperature $\theta_{CW} = 340$ K are in sharp constrast with the low value of $T_N = 11.8$ K and indicate that magnetic interactions are strongly frustrated and are expected to generate short-range order above T_N.

So far, there are no experimental indications that the AF order in its simplest form (as in Fig. 5) exists below T_N, and its nature is more subtle. One possibility is that the magnetic order is non-collinear, with complicated spin orientations. In such a case, the low-symmetry structure could be different from the tetragonal. It is also possible that below T_N the magnetic order has only a short-range character (similar to spin ice), or the long-range order coexists with the short-range order like in the $ZnFe_2O_4$ spinel [33].

In conclusion, we suggest that while the origin of the Verwey transition in Fe_3O_4 could be understood, the nature of the magnetic order in Fe_2SiO_4 below T_N poses an interesting experimental problem. We hope that future experiments will either confirm the predictions of the present studies, or indicate necessary ingredients of a more complete theoretical treatment of this problem.

Acknowledgments

The authors thank all collaborators Mariana Derzsi, Paweł Jochym, Jan Łażewski, and Małgorzata Sternik for valuable discussions. This work was supported in part

by Marie Curie Research Training Network under contract No. MRTN-CT-2006-035957 (c2c) and by the Polish government (MNiSW) within Contract No. 541/6.PR UE/2008/7. A.M. Oleś acknowledges support by the Foundation for Polish Science (FNP) and by the Polish Ministry of Science and Higher Education under project No. N202 068 32/1481.

References

[1] P.W. Anderson, *Phys. Rev.* **102**, 1008 (1956).

[2] *Frustrated Spin Systems*, Ed. H.T. Diep, World Sci., Singapore 2004.

[3] P.G. Radaelli, *New J. Phys.* **7**, 53 (2005).

[4] S. Nizioł, *Phys. Status Solidi A* **18**, K11 (1973).

[5] P.G. Radaelli, Y. Horibe, M.J. Gutmann, H. Ishibashi, C.H. Chen, R.M. Ibberson, Y. Koyama, Y.S. Hor, V. Kiryukhin, S.W. Cheong, *Nature (London)* **416**, 155 (2002).

[6] M. Isobe, Y. Ueda, *J. Phys. Soc. Jpn.* **71**, 1848 (2002).

[7] S.-H. Lee, C. Broholm, T.H. Kim, W. Ratcliff, S.-W. Cheong, *Phys. Rev. Lett.* **84**, 3718 (2000).

[8] M. Schmidt, W. Radcliff, P.G. Radaelli, K. Refson, N.M. Harrison, S.W. Cheong, *Phys. Rev. Lett.* **92**, 056402 (2004); S. Di Matteo, G. Jackeli, C. Lacroix, N.B. Perkins, *Phys. Rev. Lett.* **93**, 077208 (2004).

[9] E.J.W. Verwey, *Nature (London)* **144**, 327 (1939).

[10] M. Iizumi, T.F. Koetzle, G. Shirane, S. Chikazumi, M. Matsui, S. Todo, *Acta Crystallogr. B* **38**, 2121 (1982).

[11] J.P. Wright, J.P. Attfield, P.G. Radaelli, *Phys. Rev. Lett.* **87**, 266401 (2001); *Phys. Rev. B* **66**, 214422 (2002).

[12] E. Nazarenko, J.E. Lorenzo, Y. Joly, J.L. Hodeau, D. Mannix, C. Marin, *Phys. Rev. Lett.* **97**, 056403 (2006).

[13] I. Leonov, A.N. Yaresko, V.N. Antonov, M.A. Korotin, V.I. Anisimov, *Phys. Rev. Lett.* **93**, 146404 (2004); H.-T. Jeng, G.Y. Guo, D.J. Huang, ibid., **93**, 156403 (2004).

[14] P. Piekarz, K. Parlinski, A.M. Oleś, *Phys. Rev. Lett.* **97**, 156402 (2006).

[15] P. Piekarz, K. Parlinski, A.M. Oleś, *Phys. Rev. B* **76**, 165124 (2007).

[16] P. Piekarz, K. Parlinski, A.M. Oleś, *J. Phys., Conf. Ser.* **92**, 012164 (2007).

[17] W. Yong, E. Dachs, A.C. Withers, *Phys. Chem. Miner.* **34**, 121 (2007).

[18] I. Choe, R. Ingalls, J.M. Brown, Y. Sato-Sorensen, *Phys. Chem. Miner.* **19**, 236 (1992).

[19] M. Derzsi, P. Piekarz, P.T. Jochym, J. Łażewski, M. Sternik, A.M. Oleś, K. Parlinski, *Phys. Rev. B* **79**, 205105 (2009).

[20] G. Kresse, J. Furthmüller, *Comput. Mater. Sci.* **6**, 15 (1996).

[21] P.E. Blöchl, *Phys. Rev. B* **50**, 17953 (1994); G. Kresse, D. Joubert, ibid., **59**, 1758 (1999).

[22] Z. Zhang, S. Satpathy, *Phys. Rev. B* **44**, 13319 (1991).

[23] J. Zaanen, G.A. Sawatzky, *J. Solid State Chem.* **88**, 8 (1990).

[24] A.I. Liechtenstein, V.I. Anisimov, J. Zaanen, *Phys. Rev. B* **52**, R5467 (1995).

[25] H.P. Pinto, S.D. Elliott, *J. Phys., Condens. Matter* **18**, 10427 (2006).

[26] K. Parlinski, Z.Q. Li, Y. Kawazoe, *Phys. Rev. Lett.* **78**, 4063 (1997); K. Parlinski, PHONON software, Cracow 2008.

[27] S.K. Park, T. Ishikawa, Y. Tokura, *Phys. Rev. B* **58**, 3717 (1998).

[28] M. Reehuis, C. Ulrich, P. Pattison, B. Ouladdiaf, M.C. Rheinstädter, M. Ohl, L.P. Regnault, M. Miyasaka, Y. Tokura, B. Keimer, *Phys. Rev. B* **73**, 094440 (2006).

[29] J.-H. Park, L.H. Tjeng, J.W. Allen, P. Metcalf, C.T. Chen, *Phys. Rev. B* **55**, 12813 (1997).

[30] J.E. Lorenzo, C. Mazzoli, N. Jaouen, C. Detlefs, D. Mannix, S. Grenier, Y. Joly, C. Marin, *Phys. Rev. Lett.* **101**, 226401 (2008).

[31] Y. Fujii, G. Shirane, Y. Yamada, *Phys. Rev. B* **11**, 2036 (1975).

[32] K. Siratori, Y. Ishii, Y. Morii, S. Funahashi, S. Todo, A. Yanase, *J. Phys. Soc. Jpn.* **67**, 2818 (1998).

[33] W. Schiessl, W. Potzel, H. Karzel, M. Steiner, G.M. Kalvinus, A. Martin, M.K. Krause, I. Halevy, J. Gal, W. Schafer, G. Will, M. Hillberg, R. Wappling, *Phys. Rev. B* **53**, 9143 (1996).